One-Color and Two-Color Resonance-Enhanced Two-Photon Ionization Studies of Benzene: Sudden Drop of Photoionization Yield at the Onset of the Third Channel Region

Teijiro ICHIMURA,* Hisanori SHINOHARA,† Kazuhiko OHASHI,†† and Nobuyuki NISHI*,††
Department of Chemisty, Tokyo Institute of Technology, Ohokayama, Meguro, Tokyo 152
† Department of Chemistry for Materials, Mi'e University, Tsu 514
†† Department of Chemistry, Faculty of Science, Kyushu University, Hakozaki 812
†† Institute for Molecular Science, Myodaiji, Okazaki 444
(Received May 13, 1991)

Benzene molecules in a supersonic jet were photoionized using a tunable (233—262 nm) pulsed dye laser, and the resonance-enhanced two-photons ionization (RE2PI) processes of the S_1 state were investigated by time-of flight (TOF) mass-spectrometric technique. Without further fragmentation of $C_6H_6^+$ ions under low laser power conditions (<20 μJ/pulse), high-resolution excitation spectra of the parent ion have been measured for the $6^1 1^n$ progression (n=0,1,2,3). The relative photoionization intensity suddenly drops at the onset of the third channel band, $6^1 1^3$. Excitations of the rotationally resolved $6^1 1^3$ and $6^1 1^2$ bands under carefully controlled low laser powers have revealed the fact that the relative intensity of the $6^1 1^3$ band (above 3rd channel) to that of the $6^1 1^2$ band (below 3rd channel) decreases with decreasing the excitation laser power. This has confirmed the idea that the ionizing process is competing with nonradiative relaxation processes at the resonant state. Two-color RE2PI excitation with the pumping (ω_1) and electrically delayed probing (ω_2=272.0 nm) lasers has given population decay rates of vibronic state longer than 20 ns. Excitation spectra of the parent ion with scanning ω_1 (241—248 nm) and those with the optically delayed (2.8—8.0 ns) fixed wavelength of ω_2 have been observed. Relative population yields for the 7^1 and $6^1 1^3$ vibronic states drastically decreased in a similar fashion to the relative fluorescence yield for the longer delayed excitation. The present RE2PI measurement of the relative population yields for selective vibronic band excitations revealed that the ionization method can detect the non-fluorescent transient species produced the optical excitation above the 3rd channel of the S_1 state of benzene.

Photophysics of the S_1 ($^1B_{2u}$) state of benzene has been extensively studied with various techniques.[1-7] Of particular interest is the so-called "third channel" process. It has been observed as a sudden decrease in the fluorescence quantum yield under collision free conditions at an excess energy of ca. 2800 cm^{-1} above the origin of S_1.[8-14] The resonance-enhanced (2+2) photon ionization technique has been applied by Murakami et al.[8] and Aron et al.[9] They reported that the MPI spectra of a benzene beam reflect exactly the two-photon absorption cross sections even at the onset of the third channel, i.e. the $14^1 1^2$ band. Achiba et al.[10] observed a simillar result with two-photon ionization-photoelectron spectroscopy. Riedle et al.[11] applied a Doppler-free two-photon fluorescence excitation spectroscopy to measure the absorption linewidth of rotational quanta of the $14^1 1^n$ progression band. They concluded that the third channel of benzene is an intramolecular vibrational redistribution due to Coriolis couplings of the rotational band to short-lived vibrational background states, since some of the rotational quanta are missing for the $14^1 1^2$ band where the excess energy above the origin of the S_1 state is 3412 cm^{-1}. Fluorescence decay measurements of each vibrational level excited with tunable picosecond pulses (224—252 nm) were carried out by Sumitani et al.[12] They observed dual exponential decays at the onset of the third channel for a static benzene gas and also under supersonic beam conditions.[13]

In a previous work[15] we have applied resonance-

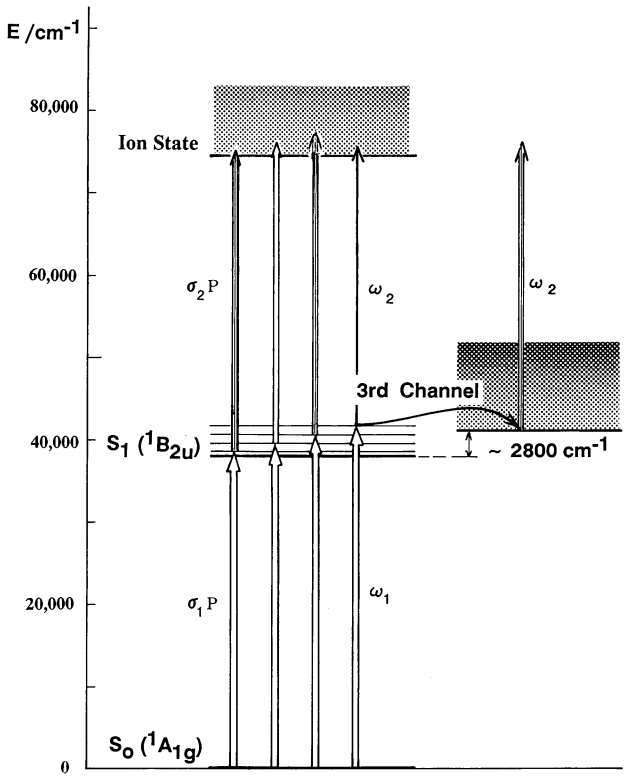

Fig. 1. A scheme of the PE2PI process of benzene around the third (3rd) channel region. Two-color RE2PI process is illustrated on the right. A laser power is denoted by P.

enhanced two-photon (1+1) ionization (RE2PI) technique to further the problem of the third chanel process of benzene. A scheme of the RE2PI process is shown in Fig. 1. One-photon resonant two-photon ionization processes involve two steps, i.e., one-photon excitation from S_0 to S_1 with a cross section σ_1 and one-photon ionizing transition from S_1 to the ionization continuum with a cross section σ_2. The cross section σ_1 is proportional to the absorption coefficient ε; which is an important characteristic of RE-(1+1)PI compared to the other REMPI's described above.

The lifetime (τ) of each S_1 vibrational level below channel three is longer than the excitation pulse width (6.5 ns) and thus a steady state condition of the S_1 state during the laser pulse can be satisfied. However, a relative decrease of the population is expected above the onset of the third channel. The isoenergetic ground state levels, internally converted from the pumped 3rd channel region, have negligibly small Franck–Condon factors to the ionization continuum.[16] The triplet state formation is not plausible for the population decay.

An evidence was presented for the decrease of the relative ion intensity in the previous work.[15] This was based upon the observation of excitation spectra of the $C_6H_6^+$ ion intensity measured over the wavelength of the $S_1 \leftarrow S_0$ transition of benzene. Reilly and Kompa[4] proposed a four-level rate equation model, which is in consequence similar to that of Fisanik et al.[17] They carried out a simulation calculation for the laser power dependence of mass integrated ion signals in KrF and ArF laser excitation of benzene. Their predicted value (ca. 20 ps) of the $^1B_{1u}$ lifetime at 193 nm seems to be quite long, which is also suggested by one of the same authors.[16]

Time-resolved RE2PI study is poweful technique to elucidate the time evolution of transient states. Duncan et al.[18] determined the triplet lifetime of benzene with pumping dye laser and a probe ArF (193 nm) excimer laser. Otis et al.[19] have applied for the first time a similar method to the channel three band. Kühlewind et al.[20] applied the method to measure dissociation rates of energy selected benzene cations formed by 2PI. Recently Schubert et al.[21] measured population decay rate of single rotational contours in the $14^1 1^2$ band above the channel three threshold. In this study we have applied nanosecond UV dye lasers to pump and probe some rovibronic bands of S_1 benzene under supersonic beam conditions (Fig. 1). The results obtained in this study will be compared with those of fluorescence quantum yields and lifetimes.

In preparing for this paper Riedle et al.[22] reported rotationally resolved spectra of the $6^1 1^3$ band. They confirmed their previous conclusion that the rotationally excited rovibronic states are thought to be coupled to background states within S_1 which are themselves broadened due to strong coupling to the highly excited S_0 electronic state.

Experimental

The apparatus for one-color and two-color resonance-enhanced two-photon ionization (RE2PI) time-of-flight (TOF) mass spectrometer has been described in detail elsewhere[23-25] and a brief description is given here. The measurements were carried out in a linear reflectron TOF mass spectrometer where a benzene molecular beam was ionized. The benzene molecular beam was formed by expanding benzene seeded in He (500 Torr—1 atm, 1 Torr=133.322 Pa) or Ar (1—2 atm) generated through a modified commercial pulsed nozzle (NRC BV-100) with 120 μs pulse duration. The pulsed beam was skimmed and introduced to the ionization region where it was crossed perpendicularly by a focused ionizing laser beam at a distance of 3 cm from the nozzle. The two laser beams in two-color experiments were collinearly aligned in opposite directions. The typical ambient pressure of the main chamber was 5×10^{-7} Torr when molecular beam running, so that the collision of the ions with back ground molecules can be neglected.

The excitation source consists of a pulsed dye laser pumped by a XeCl excimer laser (6.5 ns pulse-width). The dye laser output was frequency doubled by an auto-tracker which contains a β-barium borate (BaB_2O_4:BBO) angle-tuned crystal and Pellin–Broca prisms. In two-color experiments the output from another dye laser pumped by a XeCl excimer laser also frequency doubled by a BBO crystal and the fundamental output was removed by a filter (Toshiba UVD-33S) in this case. Since the benzene molecule was excited to S_1 in the wavelength region from 262 to 232 nm, Coumarin 500 (480—520 nm) and Coumarin 480 (460—480 nm) dyes were used to produce the corresponding frequency doubled UV laser outputs. In the case of the experiments with lower laser intensities (<10 μJ) the output power was reduced by using an appropriate filter. For the wavelength of 272.0 nm Coumarin 540A dye was used. Since the excitation at this wavelength does not produce benzene ions, higher power of the probe laser than the pumping laser was used to optimize the signal enhancement. The population decay rates of the S_1 vibronic states were determined by observing enhanced ion signals by the probe (ionizing) laser pulse irradiated after some delay time from the pump pulse. The delay time between the pump and probe pulses was varied in the range of 20—110 ns by a digital delay pulse generator or 2.8—8.0 ns by an optical delay. The resolution of dye laser pulse was 0.07 cm^{-1} without using an intracavity etalon, which is well enough to excite a rotationally resolved Q band head of a specific vibronic band in the cold beam.

Detection of benzene ions was performed by a linear reflectron TOF mass spectrometer. The linear reflectron has an ion reflector to compensate the initial velocity spread of ions in the acceleration region and thus provides high mass resolution even with present short drift length (53.6 cm). The detector at the end of the drift tube is composed of dual microchannel plates with a gain of 1×10^7. Signals from the detector were amplified and then fed to a digital storage oscilloscope, which also allows signal averaging and data transfer to a microcomputer. The microcomputer also allows for control and scanning the dye laser system. The digital delay pulse generator also controls the relative timing of the dye laser and molecular beam pulses.

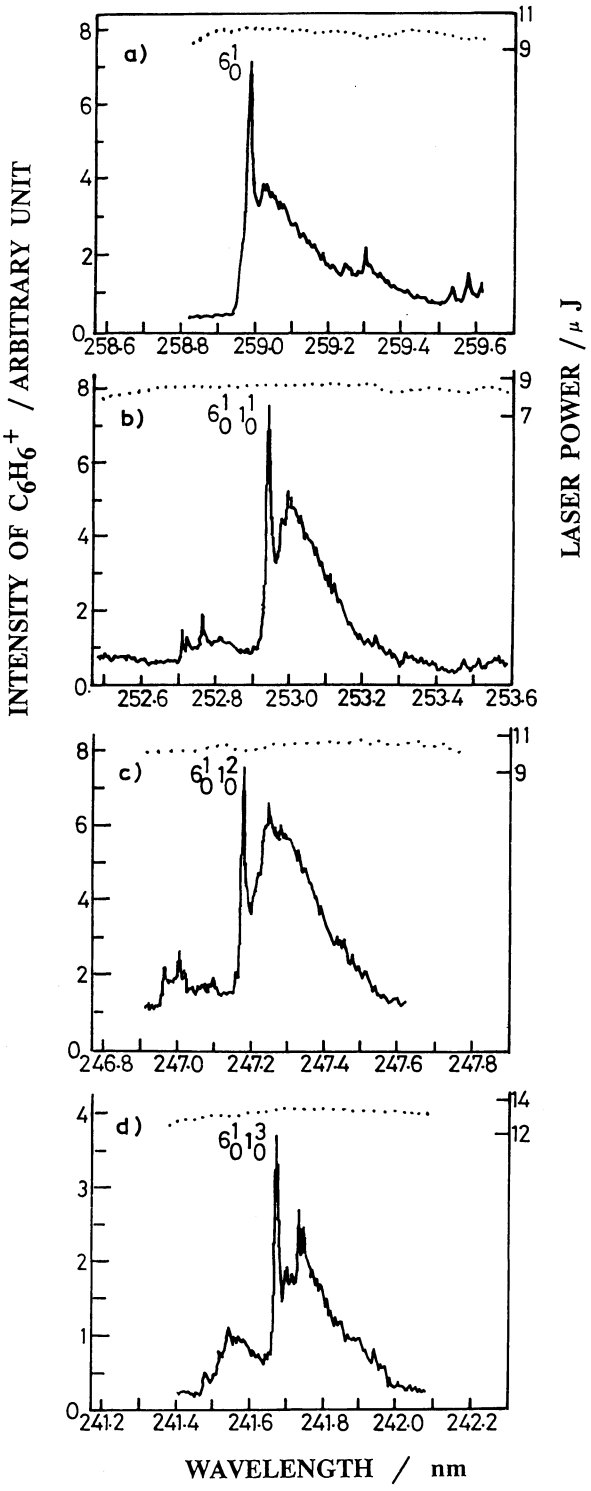

Fig. 2. High-resolution RE2PI excitation spectra of $6^1_1 1^n$ progression bands. The dotted line shows the variation of the laser output. The beam conditions were; He-seed 1 atm, nozzle temperature 36°C. The individual scans consist of 160—260 data points observed at 0.0040 nm wavelength intervals with the averaging time of 8s at 10 Hz laser repetition rate. Only prominent band heads are assigned and indicated in the figure. Observed broad bands are composed of rotationally and vibrationally hot bands due to the warm beam conditions (see text).

Results and Discussion

One-Color RE2PI Excitation Spectra of the S_1 State. A mass-tuned (m/z=78) excitation spectrum has been observed for the excitation wavelengths scanned from 235 nm to 262 nm with the laser intensity of 4—7 μJ and has already been reported in a previous work.[15] It should be noted here that the multiphoton-absorption-fragmentation of $C_6H_6^+$ is very efficient, but it can be negligibly small with the excitation laser intensities less than 20 μJ/pulse. Under these low laser powers, the observed $C_6H_6^+$ ion intensity should reflect the population density of the resonant S_1 state. The excitation spectra in the previous work,[15] however, was measured with a fairly quick scanning under warm beam conditions. Accordingly the spectral resolution was not high. As it is described in the experimental section, the present laser system has a resolution of 0.07 cm^{-1}. Therefore it is feasible to observe a high-resolution spectrum.

The excitation spectra of the $6^1_1 1^n$ progression bands at their band positions were measured under the same beam conditions as that in a previous paper,[15] but with a higher spectral resolution. The spectra are shown in Fig. 2. Some rotational envelopes of the Q blanch are observed along with some vibronic hot bands. For instance, three peaks observed at around 259.6 nm in Fig. 2-a are designated to 6^2_1 for the two of the three peaks and $6^0_1 1^2$ for the other, which have one vibrational quanta of ν_6 in the ground state. Sharp small peaks appeared at the red side of each $6^1_1 1^n$ band are assigned to be the $17^2_1 1^{n-1}$ vibronic bands by Atkinson and Parmenter.[27] Since the ion intensity below the channel 3 excitation comes from the S_1 state population,[15] the excitation spectra in Figs. 2-a, b, and c should reflect the $S_1 \leftarrow S_0$ absorption cross section. In comparison with high resolution absorption spectra at room tempsrature,[27] these spectra indicate that the resolution in this study is high enough to resolve the rotational Q band head. The beam seeded by 600 Torr (1 Torr=133.322 Pa) He should be much colder than those in Fig. 2. The Q band heads in Fig. 2 have sharp band widths of about 2 cm^{-1}. Broad rotationally hot background signals, however, seem to overlap with the Q band heads.

Ion yield for the resonant excitation in rotationally resolved Q band head was determined from the peak heights of the observed spectrum. This yield is compared with that below the channel three threshold. As described in a previous paper[15] (also cf. Fig. 1) the relative ion yield should decrease if any nonradiative process in the S_1 state occurs. The value of the $C_6H_6^+$ intensity (I) is first divided by the laser power (P) and the absorption coefficient (r), since the population in the resonant S_1 state is proportional to $N_0 \cdot r_1 \cdot P$ (N_0 stands for the S_0 population). The ratios of the intensities for the

respective vibronic bands are then normalized to that for the $6^1 1^2$ band which is below the channel three threshold. The obtained values (define $X \equiv I/P \cdot A$) from Figs. 2-a, 2-b, 2-c, and 2-d are 0.99, 0.93, 1.0, and 0.72, respectively. The X values are fairly constant for the $6^1 1^n$ progression (n=0,1,2) below the channel three threshold, but becomes smaller above the channel. The value of A (relative value of the absorption coefficient) might include some ambiguity since they were determined in a low vapor pressure (0.90 Torr) of benzene, which are essentially different from those in the molecular beam. The difference, however, is likely to be small for the values of the $6^1 1^2$ and $6^1 1^3$ bands, in comparison with those determined in cold beam conditions by Hiraya and Shobatake.[28] So it is still meaningful to compare the X values. The X value for the rotationally resolved Q band head of the $6^1 1^3$ is substantially smaller than that of the $6^1 1^2$. This trend was also seen in the low resolution spectrum obtained in the previous work,[15] indicating that the decrease in the X value is independent of spectral resolution for the excitation of the vibronic band. As it is well-known, this $6^1 1^3$ band is the onset of the third channel of benzene. The drop of the X value exactly coincides with the onset of the channel three. It is clear that the nonradiative process at the third channel is responsible for this decrease in the X value of $I(C_6H_6^+)/P \cdot A$, since the X value is inversely proportional to the nonradiative decay rate.

Cooling and Laser Power Effects on the Ionization Yields. A rotationally and vibrationally cold RE2PI excitation spectrum for the $6^1 1^2$ band is shown in Fig. 3. The cooling effect of the spectrum in Fig. 3 is clear in comparison with that observed in Fig. 2-c. The peak for the Q band head (FWHM 2.0 cm^{-1}) is well separated from the rotational hot bands. A vibronic band ($17^2 1^1$) stays on the rotational band envelope, 11.1 cm^{-1} to the red of the Q band head. The intensity of background at the band head is estimated to be less than 4% of the peak

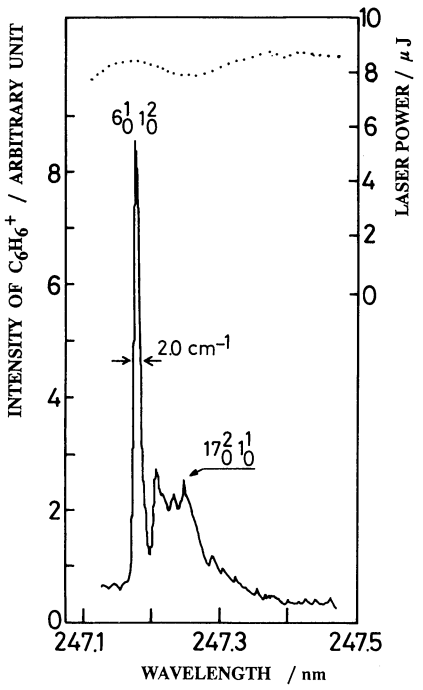

Fig. 3. Excitation spectrum of the $6^1 1^2$ band observed under the cold beam conditions (benzene vapor pressure at 0°C, seeded Ar 1 atm). The dotted line shows the variation of the laser output. The scanning rate of the excitation wavelength and the averaging time were the same as in Fig. 2. The rotational Q band head (FWHM=2.0 cm^{-1}) is well separated from other rotational bands and the vibronic band ($17^2 1^1$).

height. Under the cold beam conditions shown in Fig. 3, the C_6H_6 ion intensity for the two specific vibrational bands, i.e., $6^1 1^2$ (247.178 nm) and $6^1 1^3$ (241.675 nm), were carefully measured together with the variation of laser power (lower than 10 μJ/pulse) for the respective Q band head excitation. The peak intensities of the vibronic bands were determined by scanning the wavelength of the

Table 1. Values[a] of $X \equiv I(C_6H_6^+)/(A \cdot P)$ for Various Low Laser Powers in RE2PI of Two Specific Vibrational Band Heads $6^1 1^2$ and $6^1 1^3$ and under Cold Beam Conditions

Wavelength	Vib. band[b]	ΔE[b]	A	P	$I(C_6H_6^+)$	I_p(rel)[c]	X[d]
nm	cm^{-1}			μJ	mV		$(I/A \cdot P)$
247.178	$6^1 1^2$	2367	1.0	1.7	56	1.0	1.0
			1.0	3.7	225	1.8	1.0
			1.0	10	590	1.8	1.0
241.675	$6^1 1^3$	3291	0.48	1.7	8.0	0.29	0.29
			(0.44)			(0.32)	(0.32)
			0.48	3.7	36	0.61	0.33
						(0.66)	(0.36)
			0.48	10	190	1.2	0.67
						(1.3)	(0.72)

a) Uncertainities are ca. 10% due to experimental errors. b) Notation of the vibrational band is according to Callomon et al.[29] and ΔE indicates the excess energy above the origin band (38086 cm^{-1}).[29] c) Power dependence relative to the value at the first column. d) Values in parentheses are derived using the value of the relative absorbance (A=0.44) observed in the supersonic beam condition by Hiraya and Shobatake.[28]

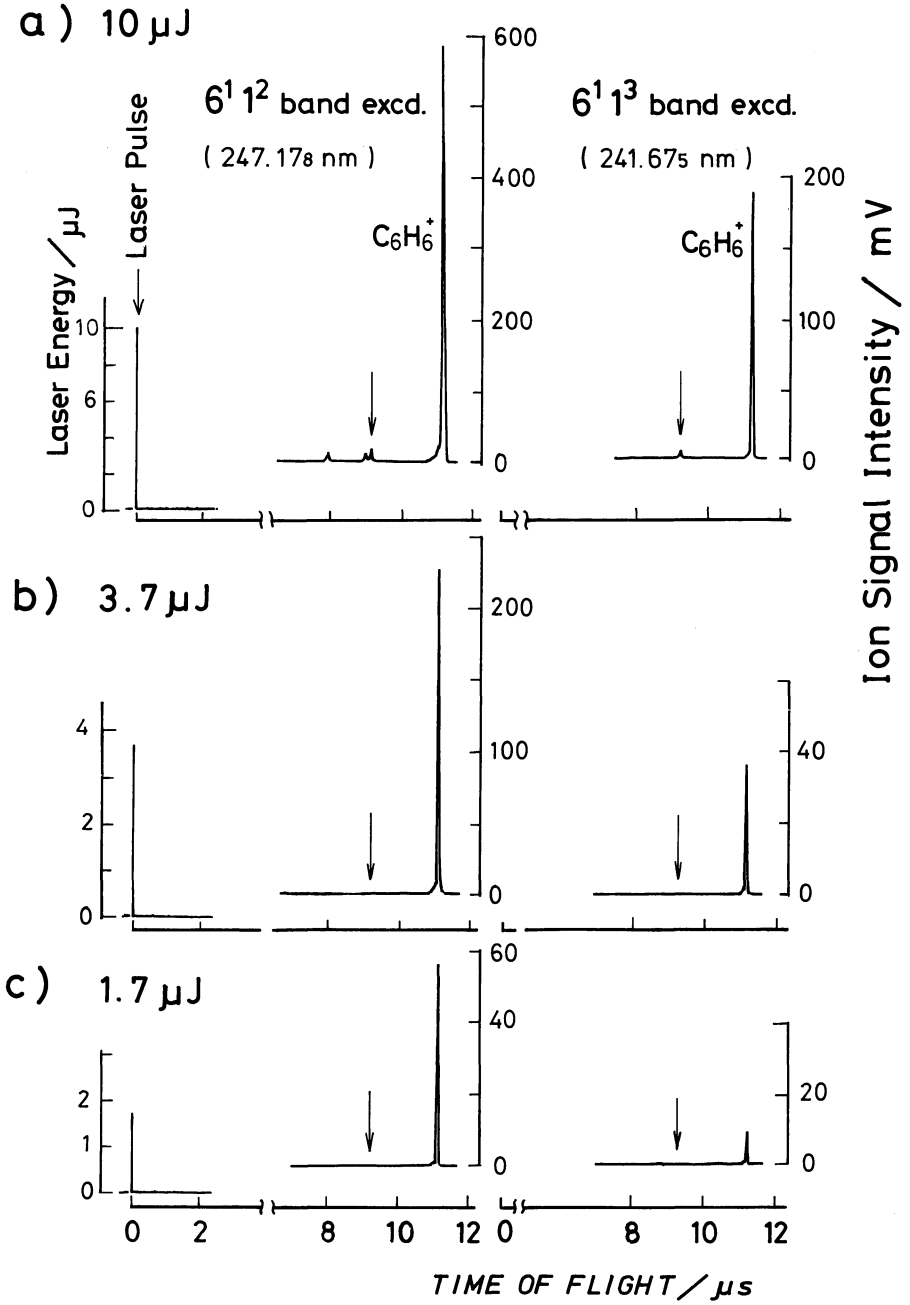

Fig. 4. RE2PI/TOF mass spectra obtained with two excitation wavelengths, 247.178 nm ($6^1 1^2$) and 241.675 nm ($6^1 1^3$) under the same cold beam conditions as in Fig. 3. Three sets of measurements were carried out for the laser intensity with 10 μJ/pulse (a), 3.7 μJ/pulse (b), and 1.7 μJ/pulse (c), where the laser intensity for set was the same. The TOF spectra shorter than 8μs are omitted in the figure. The laser intensities are also illustrated at the flight time 0. The arrow indicates the position of the $C_4H_3^+$ ion, confirming the negligible fragmentation of the parent ion $C_6H_6^+$.

dye laser. The TOF spectra taken under this condition are shown in Fig. 4 together with the laser power used. It should be noted here that the applied laser power did not cause saturation of the one-photon transition ($S_1 \leftarrow S_0$), so that the observed RE2PI signals involve information on nonradiative processes occurring at the channel three.

The derived ionization efficiencies are tabulated in Table 1. It is clear that the ratio of the X value for the Q band head excitation of the $6^1 1^3$ band to that of the $6^1 1^2$ band is decreasing with decreasing laser power. The value of 0.60 for a 6 μJ laser power obtained in our

previous work[15] indeed falls in between those for 3.7 μJ (X=0.33) and 10 μJ (X=0.67) laser powers in Table 1. The ion intensity of $C_6H_6^+$ obtained in the excitation of the rotationally resolved absorption band (Q band head) in the channel three region is quite dependent upon the excitation laser energy. The intensity decrease of the $6^1 1^3$ band is free from the variation of rotational excitation (which contributes to the background) and is due purely to the variation of the vibronic band per se. A simple power dependence shown in the second column from the right indicates that the power dependence for the $6^1 1^3$ is higher than that for the $6^1 1^2$. This can be qualitatively explained by the difference in the rates of the relaxation processes which compete with the pumping to the ion state. The relaxation rate from the $6^1 1^3$ vibronic band is much faster than that from the $6^1 1^2$ level so that the ionization via the $6^1 1^3$ level requires the absorption of the second photon within the shorter lifetime. Higher photon density supplies two photons in a shorter time window.

Two-color pump and probe method is necessary to obtain information on time evolution of the population decrease in the S_1 state. Otis et al.[19] have already applied the pump and probe (193 nm) method to elucidate the nonradiative decay rate in the $6^1 1^3$ band. We tried to do the similar method with the similar pulse width (6.5 ns) but different probe wavelength of 272.0 nm as described in the following section.

Excitation Spectra of $6^1 1^3$ and 7^1 Bands in the Cold Beam. The RE2PI excitation spectra in supersonic beam conditions were measured for 241.6—243.2 nm (Fig. 5). High resolution spectra of the $6^1 1^3$ and 7^1 bands were measured separately, but not shown in the figure. The hot background observed in Fig. 1 in our previous report[15] are totally absent for the excitation wavelength between the two bands. The rotational hot bands observed for the red side of the 7^1 band are more distinguished than those for the $6^1 1^3$ band (Fig. 5), which was much clearer in the high resolution spectra (not shown). A band contour simulation of the high resolution spectra,[30] the rotational temperature for the 7^1 band is estimated to be ca. 29 K. The relative ionization efficiency of the $6^1 1^3$ band to the 7^1 band is still similar to the value reported in our previous work.[15] In consequence, the ionization efficiency of the 7^1 band seems to be higher than those of the $6^1 1^n$ bands, which is independent of the beam conditions. This fact is inherent in the ionization step of the 7^1 band even though the ionization cross section of the band is not known at present.

Two-Color RE2PI Processes with Electric Delay Time. Two-color RE2PI with electrically delayed secondary excitation was carried out for determining the excited state lifetimes of the vibronic bands. A similar experiment was already carried out by Hopkins et al.[31] for the spectroscopic and lifetime measurements of benzene clusters. The wavelength of x_1 was tuned to the

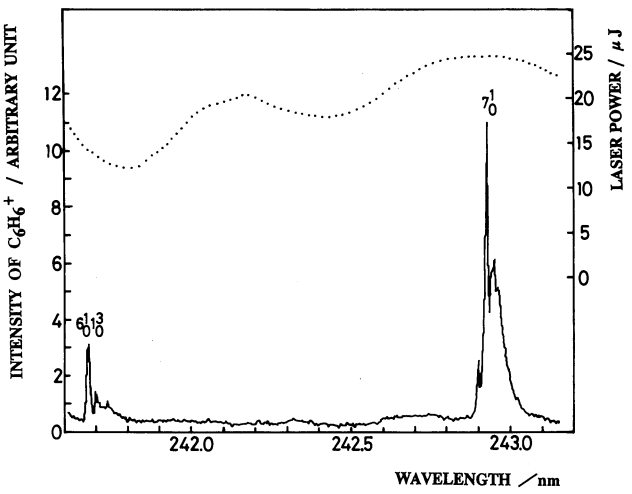

Fig. 5. RE2PI excitation spectrum of benzene in the third channel region under cold beam conditions. The dotted line shows the variation of the laser output. The beam conditions were the same as in Fig. 3. The scanning rate and the averaging time were the same as in Fig. 2. The spectrum is composed of 370 data points and flat backgrounds are observed for 241.8—242.8 nm wavelength region, giving evidence of a cold beam. The values of $I/P \cdot A$ for the Q band heads of the $6^1 1^3$ and 7^1 bands in the figure has been compared with those reported in our previous work,[15] leading to the similar ratio. The high resolution excitation spectra of the $6^1 1^3$ and 7^1 bands such as that in Fig. 3 were also observed, but not shown in the figure. The feature of the rotational hot bands was the same as in this figure.

Q band head (258.992 nm) of the 6^1 band at first. The low output energy (2—3 μJ/pulse) of ω_1 caused weak $C_6H_6^+$ ion signal due to one-color RE2PI. The following ω_2 irradiation with some delay time produced the second $C_6H_6^+$ ion signal in the TOF spectrum with the exact delay time between ω_2 and ω_1. Thus the second peak is attributed to the ionizing process by ω_2, which reflects the population decay of the resonant S_1 state pumped by ω_1.

The wavelength of ω_1 was then tuned to the Q band head of 6^1, $6^1 1^2$, 7^1, $6^1 1^3$, $6^1 10^2 1^2$, and $7^1 1^1$ bands. Enhancements of the signals by ω_2 for the 6^1, $6^1 1^2$, and 7^1 band excitations were observed, while no distinctive delayed signal appeared for the excitation of the other bands including the $6^1 1^3$ band. The lack of enhancement by ω_2 gives the upper limit of 20 ns (which is the limit caused by the firing jitter of the two excimer laser pulses) for the relaxation time of these bands.

Population decay of the pumped S_1 state could be derived from the probed ion signal intensity by delayed ω_2 irradiation. The logarithmic values of the probed intensities are plotted against the delay time between ω_1 and ω_2 as shown in Fig. 6. These plots give straight lines, of which slopes provide population decay rates.

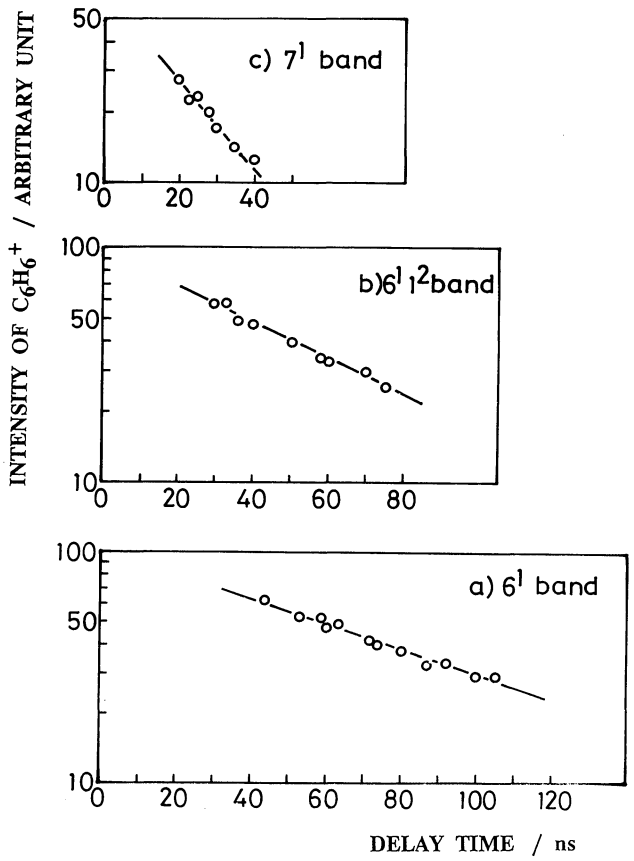

Fig. 6. Logarithmic plots of $C_6H_6^+$ ion intensities by two-color ($\omega_1+\omega_2$) irradiation against the delay time between ω_1 and ω_2. The enhanced $C_6H_6^+$ ion signals due to the two-color process were plotted for the delay time between ω_1 and ω_2, where wavelengths of ω_1 were 258.992 nm (a), 247.178 nm (b), and 242.923 nm (c), respectively. These wavelengths correspond to the rotational Q band head (FWHM=2.0 cm^{-1}) of the 6^1, $6^1 1^2$, and 7^1 bands, respectively.

Obtained population decay rates of some vibronic bands are listed in Table 2. The value for the 6^1 band (last column in Table 2) agreed with the reported value determined by a similar experiment.[31] Derived values for $6^1 1^2$ and 7^1 bands are in good agreement with those obtained by fluorescence decay measurements[12] using picosecond laser pulses. The shorter decay component (4.2 ns) of the 7^1 band was not observed due to the limited time resolution. That can be determined by an optical-delay experiment as described in the following section. In consequence the good agreement for the 7^1 vibronic state gives evidence that the present pump and probe method is applicable to determine the population decay rate of benzene longer than 20 ns. Decay rates for channel three bands, however, seem to be beyond the time resolution of the present apparatus and only the upper limit value of 20 ns can be given in the table. In order to obtain information on the decay rates of the channel three bands (7^1 and $6^1 1^3$ in particular), we have

Table 2. Population Decay Rates of Some Vibronic Levels above and below the Channel Three of Benzene Probed by Different Methods

Ex. $h\nu$/nm	Vib. band[a]	ΔE[a] cm^{-1}	τ[a] ns	This study (τ/ns)
259.0	6^1	525	81.5	75±8
247.1	$6^1 1^2$	2367	54	54±8
242.8	7^1	3080	4.2, 19.6	22±4[c]
241.7	$6^1 1^3$	3291	<0.5, 3.2	<20[c]
240.2	$6^1 10^2 1^2$	3538	<0.5, 1.0	<20
237.5	$7^1 1^1$	4001	<0.5	<20

a) Notation of the vibrational band is according to Callomon et al.[29] and ΔE indicates excess energy above the origin (38086 cm^{-1})[29] of S_1. b) Decay times taken from Refs. 12 and 31. c) See Table 3.

conducted optical-delay (<10 ns) type two-color experiments.

Optically Delayed Two-Color RE2PI Excitation. Optical delay time between ω_2 and ω_1 (produced from the two dye lasers pumped by a single excimer laser) was first set at 2.8 ns, which is shorter than the laser pulse width (8 ns). The $C_6H_6^+$ ion intensity due to one color RE2PI of the $6^1 1^3$ band was indeed enhanced with irradiation of ω_2 at 2.8 ns delayed time. This fact suggests that time-resolved ionization processes at a nanosecond time range is observable in terms of enhanced ion intensity by the present measurement. However, the exact ionization rate by one-color ω_1 pulse within 6.5 ns duration is not known and moreover the enhanced ionization rate by ω_2 within overlapped pulse time with ω_1 is also unknown. The enhancement of the $C_6H_6^+$ signal with ω_2 irradiation was much distinguished for the $6^1 1^2$ band excitation than for the $6^1 1^3$ band excitation. In the present two-color experiments, the enhancement must reflect the population of the resonant state at the fixed delay time.

The excitation spectrum of the $C_6H_6^+$ ion intensity has been measured with irradiation of scanning ω_1 and optical-delayed irradiation of ω_2. Two typical cases for different delay times are shown in Fig. 7. Relative ion intensities of the 7^1 and $6^1 1^3$ bands to that of $6^1 1^2$ band decreases remarkably with increasing the delay time from 2.8 ns (Fig. 7-a) to 8.0 ns (Fig. 7-b). The ion intensity ratio of the $6^1 1^3$ band to that of the $6^1 1^2$ band at 2.8 ns delay is much smaller than that observed in one-color RE2PI experiment. This is indicative of the fact that the lifetime in the $6^1 1^3$ state is shorter than 2.8 ns as is given in Table 2. It should be emphasized that due to the low laser power of ω_1 (less than 1 μJ/pulse), contribution from the one-color RE2PI process can be negligible. The fluctuation of the power through the scanning of ω_1 was at most 25%, and was taken into account to determine the population yield. The intensity of ω_2 was 15 μJ/pulse and kept constant throughout the two-color RE2PI excitation experiment. Therefore the ion intensity decrease observed in Fig. 7-b can be attributed solely to the population decrease of the

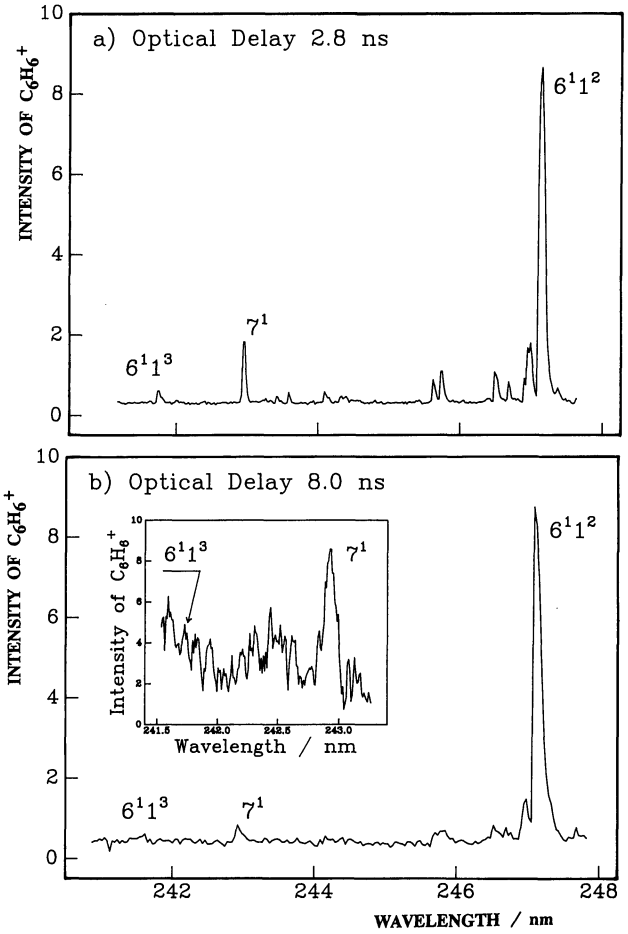

Fig. 7. 2C-RE2PI excitation spectrum of the parent ion with two different optical delay times between ω_1 and ω_2; (a) 2.8 ns delay and (b) 8.0 ns delay. The beam conditions were; Ar-seed 2 atm, nozzle temperature 46°C. The beam conditions were the same for the two experiments, but the background in the spectrum (a) was more smooth than in (b). The laser power of ω_1 was less than 1 μJ/pulse, neglecting one-color RE2PI processes. The wavelength of ω_2 was fixed at 272.0 nm and its power was approximately 15 μJ/pulse and kept constant throughout scanning of ω_1. The individual scans consist of 300 data points observed at 0.002 nm wavelength intervals with the averaging time of 8 s at 10 Hz laser repetition rate. For 8.0 ns delay experiment the signal for the third channel region was very weak and the excitation spectrum in the region 241.5—243.3 nm was separately observed with higher sensitivity than the case in (a). The spectrum is shown in the inset. The relative values of peak heights and areas observed in the spectra (a) and (b) were used in Table 3.

resonant vibronic state. The relative population yields of the resonant state can be derived in analogy to the derivation of the relative ion yield described in the earlier section. The obtained relative population yields ($X(t) \equiv I(t)/P \cdot A$) and the derived population decay times (τ) for the 7^1 and $6^1 1^3$ band excitations are summarized in Table 3.

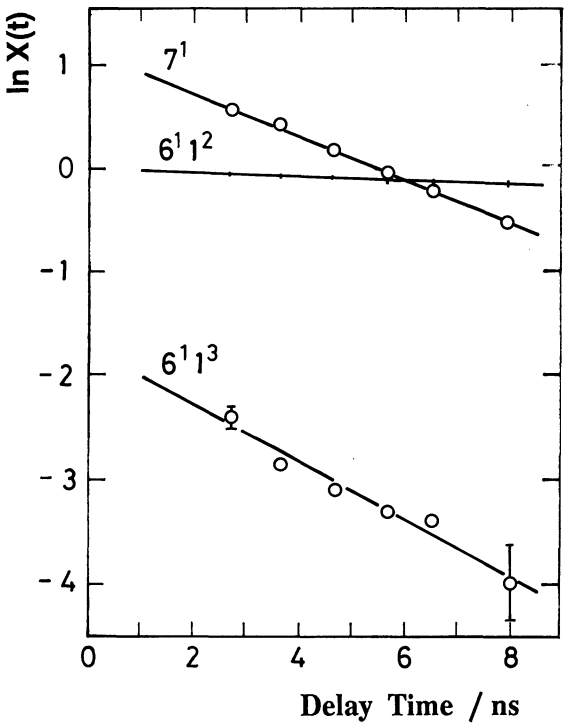

Fig. 8. Natural logarithmic plots of $X(t)$ against the delay time. The value of $X(t)$ is defined as the relative population yield to that of the $6^1 1^2$ band at the delay time $t=0$. $X(t)$ values obtained by six different delay time measurements of 2C-RE2PI excitation spectra including two scans in Fig. 7 are indicated circles, two of which indicates the experimental error bar. Solid lines show the least square fit of the data using the relation, $X(t)=X_0 \exp(-t/\tau)$. The slope of the straight lines lead to the values of τ. The line for the $6^1 1^2$ band excitation is drawn by the assumption that the value of τ is 54 ns taken from the result in Table 2.

In Table 3 relative fluorescence quantum yields (Φ_f) and X values by one-color RE2PI experiments are also listed for comparison. Both the fluorescence and relative population yields are normalized to 1.0 for the values of the $6^1 1^2$ band resonant excitations. As is clearly shown, the population yield of the $6^1 1^3$ band excitation drastically drops with increasing the delay time in a similar fashion to the fluorescence yield. The value of the population yield at 8.0 ns delay time seems to be equivalent to the fluorescence yield, though the peak intensity of the $6^1 1^3$ band signal is very weak and then is estimated to be equal to or less than the noise level. In Table 3 the population decay times (τ) listed in the last column were derived from the fitting of X values under the assumption that the X values observed at different delay times are obedient to a single exponential decay function (namely, $X(t)=X_0 \exp(-t/\tau)$). Logarithmic plots of X values against the decay time τ indeed have given a straight line (Fig. 8), of which slope gave the value of τ. The decay seems to be composed of dual exponential functions, but the approximation must be

Table 3. Relative Population Yields of Two Vibronic Levels in the Channel Three Region of Benzene Probed by Three Different Methods and Decay Times Derived from the Pump and Probe Method in This Study

Vib. band	ΔE[a] / cm^{-1}	Φ_f[b]	One color RE2PI[c]	$X(t)$ by 2C-RE2PI[d] t=2.8—8.0 ns	τ (decay time)[e] / ns
$6^1 1^2$	2367	1.0	1.0	0.95 —0.86	54
7^1	3080	0.08	2.6	1.7 —0.57	4.6
$6^1 1^3$	3291	0.014	0.67—0.29	0.091—0.018	3.5

a) Excess energy above the origin (38086 cm^{-1})[29] of S_1. b) Relative fluorescence quantum yields taken from Ref. 12. c) Relative value of X obtained by one-color RE2PI taken from our Ref. 15 and also from Table 1. d) Uncertainties are ca. 10% due to experimental errors except for that (ca. 50%) for the value of 0.018. The values obtained from the peak heights and the peak areas such as in Fig. 7 are normalized to 1.0 for the $6^1 1^2$ band excitation at delay time t=0 (X_0=1). e) The decay time (τ) is derived from the slope of the straight line in Fig. 8 with $X(t)=X_0 \exp(-t/\tau)$. The value (54 ns) for the $6^1 1^2$ band excitation is taken from Table 2.

valid within the limited time range of 2.8—8.0 ns for the fitting. The decay for the 7^1 band excitation is practically dual, one (ca. 22 ns) is obtained by the electric delay experiment (Table 2) and the other (4.6 ns) is determined from this optical delay experiment. These lifetimes are in good agreement with a previous report[12] (Table 2).

The decay for the $6^1 1^3$ band excitation was also reported to have dual exponential functions[12] as listed in Table 2. The present study (based on the above analysis) led to derivation of nanosecond decay rate of the $6^1 1^3$ vibronic state and the obtained value (3.5 ns) is in accord with the fluorescence lifetime (3.2 ns).[12] The value also agrees with the average of the decay rates for the rotational Q branch of the $6^1 1^3$ band recently reported by Riedle et al.[22] Since the present excitation resolution is 0.07 cm^{-1}, the value should correspond to the ensemble for these rotational contours included within the band width. From the results in Table 3 we may conclude that two-color RE2PI spectroscopy employed in this study is also applicable to elucidate a few nanosecond time evolution of nonradiative processes occurring in channel three vibronic states of benzene. The obtained decay time of 3.5 ns for the $6^1 1^3$ vibronic state indicates that the excited molecules in the vibronic state are subjected to the fast radiationless processes.

The value of X_0 for the $6^1 1^3$ band excitation is found to be 0.18, which is an extrapolated $X(t)$ value at time t=0. This value is eventually similar to the X value of one-color RE2PI with the lowest energy of 1.7 μJ and so is the X_0 value for the 7^1 band excitation. Both the $6^1 1^3$ and 7^1 states have dual exponential decay functions and those decay rates for the 7^1 state were determined from the present two-colors experiments. However, a faster decay rate for the $6^1 1^3$ state (Table 2) could not be derived from the present study. Only the existence of the faster decay process than the probed 3.5 ns one is confirmed by the fact that the X_0 for the $6^1 1^3$ state is much less than the unity, namely the normalized X_0 value. The fast decay process seems to be the transition to the unknown transient state. To clarify this unknown transient state one must proceed to do the two-color RE2PI experiment using two picosecond or femtosecond laser systems.

Detectability of Non-Fluorescent Transient Species by Ionization Method. In regard to quantitative discussion on the results in Tables 1, 2, and 3, the one-color RE2PI method may lead to the similar results as in fluorescence quantum yield measurements, since the ionizing transition in the RE2PI process is competing with nonradiative processes occurring at the resonant vibronic levels of the S_1 state of benzene. As far as the short lifetime of the $6^1 1^3$ state is concerned, the second photon ionization in the one-color RE2PI process should occur within the laser-pulse duration time. Thus the ion intensity may reflect somewhat time-integrated value. However, the X value of the $6^1 1^3$ band relative to that of $6^1 1^2$ is 0.29—0.67 even for the lowest power of 1.7 μJ/pulse and this value is 2.3—5.4 times higher than the X value of 0.12 (for the 6.5 ns pulse excitation) expected from the relative fluorescence quantum yield (0.014).[12] The ionization method can excite non-fluorescent "transient" species generated through the nonradiative transition from the primarily prepared fluorescent states. This non-fluorescent transient species, however, should have an ionization energy lower than or similar to that of the fluorescent species for one (or two) more photon ionization from the prepared state. Therefore, if the electronic structure of the transient species changes producing a new "transient" species (due to some geometrical change) and its ionization requires energy much higher than the two-photon energy, then the non-fluorescent transient states cannot be detected any more by this method. The detectable transient state cannot be a vibrationally hot ground state, since the internally converted state have negligibly small Franck–Condon factor to the ionization continuum.[16] It is possible for a triplet state to be ionized, but that is a minor contribution to the ionization yield.[19] Results of fluorescence spectroscopy[12,13] suggested that the fast decay is not an IVR but more likely the transition to the unknown precursor to give an isomer. Although it is not possible to identify the character of the fast decay process from the present results, the relatively large X value may include

ionization of this unknown state. The detectability of non-fluorescent transient species is an important feature characteristic of the RE2PI process compared to the fluorescence spectroscopy.

Conclusion

The occurence of the fast nonradiative process in the third channel region of benzene was probed by the observation of the decrease of ionization efficiency above the channel three threshold relative to that below the threshold in the RE2PI excitation spectrum. The relative intensity decrease is independent of the rotational temperature of the molecular beam, but is dependent upon the laser power of the RE2PI process.

The relative intensity decrease has been measured with two-color RE2PI (pump and probe) technique. Electrically delayed experiments determined population decay rates of some vibronic bands longer than 20 ns. With optical delay experiments a few nanoseconds decay rates for 7^1 and $6^1 1^3$ states in the 3rd channel region were determined and these values are in good agreement with those obtained by fluorescence decay measurements using picosecond pulses. Relative population yield of the $6^1 1^3$ state extrapolated to $t=0$ ns is much less than that of the $6^1 1^2$ state, revealing the existence of much faster decay process at the $6^1 1^3$ state than a few nanoseconds.

References

1) C. S. Parmenter, *Adv. Chem. Phys.*, **22**, 365 (1972).
2) L. D. Ziegler and B. S. Hudson, "Excited States," ed by E. C. Lim, Academic Press, New York (1982), Vol. 5, pp. 41—140.
3) M. A. Duncan, T. G. Dietz, and R. E. Smalley, *J. Chem. Phys.*, **75**, 2118 (1981).
4) J. P. Reilly and K. L. Kompa, *J. Chem. Phys.*, **73**, 5468 (1980).
5) R. B. Bernstein, *J. Phys. Chem.*, **86**, 1178 (1982).
6) K. P. Gross, D. M. Guthals, and J. W. Nibler, *J. Chem. Phys.*, **70**, 4673 (1979).
7) R. A. Covelskie, D. A. Dolson, and C. S. Parmenter, *J. Phys. Chem.*, **89**, 645 and 655 (1985).
8) J. Murakami, K. Kaya, and M. Ito, *J. Chem. Phys.*, **72**, 3263 (1980).
9) K. Aron, C. Otis, R. E. Demaray, and P. M. Johnson, *J. Chem. Phys.*, **73**, 4167 (1980).
10) Y. Achiba, A. Hiraya, and K. Kimura, *J. Chem. Phys.*, **80**, 6047 (1984).
11) E. Riedle, H. J. Neusser, and E. W. Schlag, *J. Phys. Chem.*, **86**, 4847 (1982).
12) M. Sumitani, D. V. O'Connor, Y. Takagi, N. Nakashima, K. Kamogawa, Y. Udagawa, and K. Yoshihara, *Chem. Phys.*, **93**, 359 (1985).
13) M. Sumitani and K. Yoshihara, Symposium on Molecular Structure, Kanazawa, October 1987.
14) T. Suzuki and M. Ito, *J. Chem. Phys.*, **91**, 4564 (1989).
15) T. Ichimura, H. Shinohara, and N. Nishi, *Chem. Phys. Lett.*, **146**, 83 (1988).
16) E. Sekreta, K. G. Owens, and J. P. Reilly, *Chem. Phys. Lett.*, **132**, 450 (1986).
17) G. F. Fisanik, T. S. Eichelberger IV, B. A. Heath, and M. B. Robin, *J. Chem. Phys.*, **72**, 5571 (1980).
18) M. A. Duncan, T. G. Dietz, M. G. Liverman, and R. E. Smalley, *J. Phys. Chem.*, **85**, 7 (1981).
19) C. E. Otis, J. L. Knee, and P. M. Johnson, *J. Chem. Phys.*, **78**, 2091 (1983).
20) H. Kuhlewind, E. Riedle, H. J. Neusser, and E. W. Schlag, *J. Phys. Chem.*, **88**, 6104 (1984).
21) U. Schubert, E. Riedle, H. J. Neusser, and E. W. Schlag, *J. Chem. Phys.*, **84**, 6182 (1986).
22) E. Riedle, Th. Weber, U. Schubert, H. J. Neusser, and E. W. Schlag, *J. Chem. Phys.*, **93**, 967 (1990).
23) H. Shinohara and N. Nishi, *Chem. Phys. Lett.*, **141**, 292 (1987).
24) H. Shinohara and N. Nishi, *Chem. Phys.*, **129**, 149 (1989).
25) H. Shinohara and N. Nishi, *J. Chem. Phys.*, **91**, 6743 (1989).
26) H. J. Neusser, *Int. J. Mass Spectrom. Ion Phys.*, **79**, 141 (1987).
27) G. H. Atkinson and C. S. Parmenter, *Mol. Spectrosc.*, **20**, 20 (1976).
28) A. Hiraya and K. Shobatake, *J. Chem. Phys.*, **94**, 7700 (1991).
29) J. H. Callomon, T. M. Dunn, and I. M. Mills, *Philos. Trans. R. Soc. (London), Ser. A*, **259**, 499 (1966).
30) H. Shinohara, T. Ichimura, and N. Nishi, unpublished results.
31) J. B. Hopkins, D. E. Powers, and R. E. Smalley, *J. Phys. Chem.*, **85**, 3739 (1981).